Lidar-Derived Forest Metrics Predict Snow Accumulation and Ablation in the Central Sierra Nevada, USA

Cara R. Piske[1], Rosemary Carroll[2], Gabrielle Boisrame[2], Sebastian A. Krogh[3], Aidan L. Manning[4], Kristen L. Underwood[5], Gabriel Lewis[4], and Adrian Harpold[4]

[1]Airborne Snow Observatories Inc
[2]Desert Research Institute
[3]Universidad de Concepcion
[4]University of Nevada Reno
[5]University of Vermont

June 10, 2024

Abstract

Snowmelt is a critical water resource in the Sierra Nevada impacting populations in California and Nevada. In this region, forest managers use treatments like selective thinning to encourage resilient ecosystems but rarely prioritize snowpack retention due to a lack of simple recommendations and the importance of other management objectives like wildfire mitigation and wildlife habitat. We use light detection and ranging (lidar) data collected over multiple snow accumulation seasons in the Sagehen Creek Basin, central Sierra Nevada in California, USA, to investigate how snowpack accumulation and ablation are affected by forest structure metrics at coarse, stand-scales (e.g., fraction of vegetation, or fVEG) and fine, tree-scales (e.g., a modified leaf area index, and the ratio of gap-width to average tree height). Using a newly developed lidar point cloud filtering method and an "open-area reference" approach, we show that for each 10% decrease in fVEG there is a ~30% increase in snow accumulation and a ~15% decrease in ablation rate at the Sagehen field site. To understand variability around these relationships, we use a random forest analysis to demonstrate that areas with fVEG greater than ~30% have the greatest potential increased accumulation response after forest removal. This spatial information allows us to assess the utility of completed and planned forest restoration strategies in targeting areas with the highest potential snowpack response. Our new lidar processing methods and reference-based approach are easily transferrable to other areas where they could improve decision support and increase water availability from landscape-scale forest restoration projects.

Introduction

Mountain snowpacks serve as natural water towers, dictating the timing of peak soil moisture, controlling evapotranspiration dynamics, and sustaining streamflow into the dry summer months . A warming climate suggests a future with increased precipitation variability and a decrease in snowpack accumulation and retention . Climate change has also affected frequency and magnitude of disturbances from fire, insects, and drought in forested areas that are seasonally snow covered. Montane forest ecosystems across the western U.S. are particularly vulnerable to these shifting snow dynamics because they have historically relied on snowmelt to support water demand during the growing season . The Sierra Nevada mountains, for example, have a snow-dominated precipitation regime and supply over half of California's water needs . In the Sierra Nevada, efforts are underway to introduce low-to-moderate severity fires and selective thinning to create forest conditions that promote ecosystem function resembling historical, pre-fire suppression conditions . A

knowledge gap in predicting the effects of forest disturbance on snow retention is limiting forest managers' ability to contend with current and future water supplies .

Precipitation patterns are typically the primary control on snowpack accumulation, while energy input patterns normally dictate ablation; however, terrain and vegetation characteristics serve as secondary controls (. In most locations, orographic precipitation causes deeper snowpacks at higher elevations with limited redistribution of snow by wind . North-facing slopes in the northern hemisphere receive less radiation, particularly during the winter months when sun angles are lower. Therefore, higher elevation, steeper, and more northern-facing slopes in the Sierra Nevada typically both accumulate and retain more snow .

Predicting snow response to forest canopy (and its removal) remains challenging, despite decades of research, because of complex inter- and counter-acting processes controlling the surface energy and water budget . Snowfall is intercepted in forest canopies, where it sublimates rapidly, but predictions of snow interception are uncertain . In warmer regions with minimal wind redistribution, like the Sierra Nevada, up to 60% of precipitation can be intercepted and sublimated from the forest . Forest canopy also changes wind patterns, reducing snow redistribution and changing turbulent heat fluxes , and alters radiation fluxes by both shading the snowpack from shortwave radiation and emitting longwave radiation (Lundquist et al., 2013; Safa et al., 2021). Shortwave radiation typically dominates energy fluxes available for snow ablation in the Sierra Nevada, but longwave radiation from forests is more important when solar irradiance is low and air temperatures are warmer . The interplay between long and shortwave radiation inputs in the winter and spring - when solar irradiance is relatively low - causes snow to ablate more quickly and disappear earlier under forest canopy in warmer places like the Sierra Nevada . However, the impact of forest canopy loss on snow ablation rates across complex topography is not well understood because it cannot be captured well by point-scale or coarser remote sensing and because we lack consistent methodology using newer fine-scale remote sensing.

Forest effects on snow accumulation and ablation are well documented, yet a cohesive framework for predicting forest disturbance effects on snow is lacking . Early studies in the Sierra Nevada showed that forests with open glades accumulated more snow than dense forest patches (Church, 1933; Anderson, 1956, 1963). Varhola et al. (2010) showed through a meta-analysis that reducing the fraction of area covered by forests (fVEG) promoted accumulation, while ablation showed the opposite trend. Their synthesis of 30 studies had large uncertainties that cannot be attributed to local climate or terrain . The Varhola et al. (2010) model was based on coarse-scale forest cover information; however, recent evidence shows that fine-scale forest structure metrics, like tree-scale forest gaps , forest clumps, edges of different vegetation density, and tree height , are critical to simulating larger scale snow distributions and amounts . The methodological framework used by Varhola et al. (2010), which used an open reference site approach, remains a current predictive paradigm but does not utilize information on fine-scale forest structure. Studies commonly focus on binary canopy classifications (i.e., open/ closed) or coarser scale (10-1000 m^2) fractional canopy metrics to investigate forest-snow interactions as opposed to finer scale (1-30m^2) metrics that classify vegetation structure and density (e.g., leaf area index, or LAI) as well as gap characteristics (e.g., ratio of vegetation heigh to gap size, or openness) .

Fine-scale forest structure and snow information from airborne light detection and ranging (lidar) data have revolutionized our understanding of snow-forest interactions , but remain underutilized for predicting forest management effects on snowpack. Lidar offers substantial advantages over other remote sensing tools because emitted light pulses can penetrate vegetation canopy and be used to create spatially distributed models of the ground/snow surface, canopy height, and canopy density at a decimeter-scale accuracy over extents greater than 100 km^2 . An influx of lidar datasets from initiatives like SnowEX and organizations like the Airborne Snow Observatories, Inc. (ASO) and the National Center for Airborne Laser Mapping (NCALM) present unique opportunities to take advantage of high-resolution spatially distributed data with increasing temporal distribution. However, there are few consistent processing methods to resolve snow depth and snow water equivalent (SWE) from lidar in dense forests due to various complications. For example, the number of returns is reduced due to interactions with dense vegetation, low branches can be confounded with the snow surface, and variable snow density adds spatial heterogeneity (both vertically throughout the snowpack and

horizontally over the landscape). Moreover, large-scale processing of dense point clouds is computationally intensive and requires expert knowledge of vertical and lateral biases typical in these datasets . Developing a consistent and open-source, lidar-based tool to estimate the effects of vegetation on snow accumulation and ablation has been the focus of the scientific and forest management community for the last several years . Existing decision support tools show varied results when applied at different scales and no current product effectively utilizes snow depth lidar datasets that are becoming increasingly available .

Taking advantage of a unique set of lidar datasets from the densely forested Sagehen Creek Basin in the central Sierra Nevada, California, we investigate how forest structure metrics interact with terrain to control snowpack accumulation and retention. Ongoing management in this study area includes the introduction of low to moderate severity fires and selective thinning to create more resilient forests . There is promise for increasing hydrological outputs from restoring forests, including an increase in snowmelt magnitude and streamflow . We develop a novel method for processing multitemporal lidar datasets to examine patterns over complex topography and heterogenous forest canopy. We pose the following questions:

How does coarser-scale fractional canopy cover influence snow accumulation and ablation as predicted by the current Varhola et al. (2010) paradigm?

What role do terrain (elevation, aspect, and slope) and finer-scale vegetation structure (openness) play on snow accumulation and ablation?

Beyond addressing these questions, a primary goal of this study is to create a replicable, open-source workflow to process point clouds into novel snow and canopy metrics. Our work serves as an important proof-of-concept for a new lidar-based method to develop local forest information relevant to decision support needed in forest restoration planning.

Methods

Study Site

Sagehen Creek Basin (SCB), located in the eastern Sierra Nevada, spans 28 km^2 and roughly 1800-2650 meters in elevation. The study domain is about 7 by 8 km, extending beyond the watershed (Figure 1). SCB has a unique record of research spanning more than 50 years . SCB sits within the Sierran Steppe-Mixed Forest-Coniferous Forest-Alpine Meadow Province, and dominant vegetation types include Jeffrey Pine (P. jeffreyi), Lodgepole Pine (Pinus contorta), Ponderosa Pine (P. ponderosa), Red Fir (A. magnifica), Sugar Pine (P. lambertiana), Western White Pine (P. monticola), and White Fir (Abies concolor) . The Mediterranean climate in this region has warm, dry summers and cold, wet winters. Precipitation is dominated by snow . There are three snow telemetry (SNOTEL) sites within or directly surrounding the basin (http://www.wcc.nrcs.usda.gov/snow/) which measure depth and SWE using snow pillows. Median peak SWE ranges from 37 cm at the lowest SNOTEL site (Station name: Independence Creek; Station ID: 540, elevation 1961 m) to 113 cm at the highest site (Station name: Independence Lake, Station ID: 541, elevation 2541 m). The mean 30-year winter (DJF) temperature ranges from -1.7°C to -1.8°C from the lowest to highest SNOTEL site (Figure 1).

The ecohydrology of SCB since ˜1200 CE has been shaped by anthropogenic influences. Indigenous forest management (e.g., prescribed burns), primarily influenced by the presence of the Washoe (Wá[?]šiw) Tribe, formed a heterogeneous ecosystem from ˜1200 CE until the mid-19^{th} century with fire return intervals around two years . Subsequent settlement led to a period of timber harvesting until the early 20^{th}century and fire suppression thereafter. This suppression resulted in dense, homogenous forests susceptible to high-intensity disturbance (e.g. wildfire, drought; . The "Sagehen Fuels Reduction Project" (Sagehen Project), a collaborative effort aimed at restoring and enhancing ecological heterogeneity and resilience to wildfires, has had a substantial impact on the landscape of SCB. Fuel treatments, including prescribed burns and forest thinning, were implemented at target sites in the late 2010s (Figure 1c). The goal of these management

initiatives was to restore ecosystem function and enhance species conservation. However, less is known about how these treatments, or landscape disturbances, explicitly influence hydrological processes driven by snowmelt .

Lidar Data and Processing

Lidar is an active remote sensing tool that emits pulses of light at near infrared wavelengths (typically 1064 nm). At the target scales for this study (individual tree to hillslope), lidar data is collected using instruments aboard fixed-wing aircrafts. Full waveform pulses are emitted from lidar scanner and reflected off objects and the stronger returns are discretized into points based on the return time of the pulse. Lidar resolution is quantified as a function of ground and non-ground (e.g. vegetation) returns per square-meter (See Table A4 for resolution specifications of the data used in this study).

Major limitations of airborne lidar data are the temporal resolution and cost of acquisition, which can inhibit multiple flights. While peak SWE (historically around April 1) is typically targeted for lidar data acquisitions, SNOTEL data often reveal ablation at lower elevation sites before that date . Therefore, early lidar flights can be valuable to investigate accumulation dynamics. However, climate variability complicates the prediction of peak SWE timing, and later flights can provide more useful information to stakeholders interested in the magnitude of spring melt.

The study period covers 2008 to 2022 (Table A4), with specific dates of inquiry driven by lidar data availability. Later flights were impacted by significant ablation, particularly at lower elevations (Figure 2). Despite their temporal limitations, these data present a unique opportunity because a series of multi-temporal flights in March, April, and May 2016 captured both early and late season ablation, allowing us to take advantage of spatially distributed SWE data. Lidar data was sourced from ASO and the National Center for Airborne Laser Mapping (NCALM). Snow depth was calculated by differencing snow-on and snow-off flights. Snow-off lidar was flown by NCALM in the summer of 2014 with an average point density of 9 pts/m^2 . Snow-on lidar was flown in the early accumulation season of 2008 (on February 10) by NCALM, with an average point density 5 pts/m^2 and again in 2016 by ASO at near peak SWE (March 26), early in the ablation season (April 17), and late in the ablation season (May 18) with average point densities ~2 pts/m^2 . A second snow-off lidar was acquired by NCALM in the fall of 2020 (11/20) with an average point density of 21 pts/m^2 . Snow-on lidar post-2020 was also flown by NCALM. This flight was targeted to capture peak SWE in the spring of 2022. Early season accumulation followed by a long period of ablation shifted the peak SWE ~10 days earlier than April 1. Therefore, the data was collected on March 21 to target peak SWE with an average point density of 28 pts/m^2 .

Data processing was modified from the workflow of Kostadinov et al., 2019 (See Appendix A for more details on lidar processing) to optimize reproducibility and to enable analyses in diverse vegetation types. Vertical biases were corrected across the watershed based on available ground-truth points (Table A4; Figure A4).

After the vertical bias was corrected, we classified the snow-off vegetation using a refined classification logic (Table A1) to produce four canopy strata classes: open, short, understory, and tall (Figure 3). In addition, an open reference class represents open areas with a 1 m buffer around the canopy to mitigate edge effects for our analyses (Figure A5). Snow depth was calculated by taking the height above ground and filtering based on the canopy strata classifications (Table A2). Snow density was modeled using the Snow Physics and Lidar Mapping (SnowPALM) model, which calculates compaction as a function of albedo and snow density decay using values calibrated from SNOTEL sites, as well as the effect of canopy interception and sublimation of snowfall, shortwave transmittance through the canopy, and longwave radiation emitted by the forest, and the full energy balance of the snowpack . Where data was available, SnowPALM was validated against field and SNOTEL data . The median difference between SnowPALM and ground-truth snow density was <1 kg/m^3. We did not correct for this discrepancy in our final SWE calculations, since this difference is smaller than the range of spatial variability in density. The SnowPALM model calculated snow density for each water year at 1-m spatial resolution. From lidar snow depth and SnowPALM density, we calculated SWE at

1 m (pixel) and averaged that to 30 m (grid) resolution.

We chose several key terrain variables to characterize the landscape as proxies for the energy and mass-balance dynamics that control snowpack accumulation and ablation . Northness (cos(aspect) * sin(slope)) primarily represents solar radiation while eastness (sin(aspect) * sin(slope)) represents wind loading that alters mass redistribution, since the predominant wind direction is from the west. Elevation correlates with both precipitation and temperature.

Forest structure metrics were chosen to represent the wide range of classifications that are used in other studies consistent with coarse metrics (i.e. Varhola et al. 2010) and newer, lidar-based metrics of fine forest structure . See Table A3 for forest structure classification descriptions. We chose to investigate the fraction of vegetation (fVEG), a modified leaf area index (LAI'), and openness index. fVEG is a coarser-scale forest structure metric that indicates the portion of a grid cell covered by pixels with maximum canopy height greater than three meters, impacting both the incoming radiation dynamics and interception . LAI is the most consistent with previous studies used by Varhola et al. (2010) that used full "forest cover" to define dense, interacting canopies. LAI', calculated using a combination of a point density ratio and canopy height model, serves as a proxy index for the total surface area of the leaves or needles on the canopy, acting as a limiting factor for canopy interception. This metric was then scaled to the maximum forest height . Openness represents gap dynamics influencing incoming solar radiation and breaks in potential interception. We defined openness as the ratio of the gap diameter (or twice the maximum distance to nearest canopy) to the average forest height in each grid cell. We took the natural log of the openness variable so that negative values represent forest gap to average tree height ratios less than one and positive values represent forest gap to average tree height ratios greater than one .

"Open Reference Site" Analysis

The space-for-structure approach aims to control for terrain and isolate secondary vegetation impacts on snow. The primary assumption associated with this method is that the dynamics dictated by the forest structure at one location are representative of dynamics that would occur if the structure at another location shifted towards the former.

Following the methodology of Varhola et al. (2010), SWE was normalized based on a "reference" value using Equation 1, below. This normalization was calculated to control for precipitation and terrain differences across the study domain.

$$\Delta y = 100\frac{x-R}{R} \quad (1)$$

Here, [?]y represents the percent difference between the target value (x) and a reference value (R). These percent change values were calculated for several inputs. The general form of Equation 1 was used to determine how accumulation changed with increasing canopy cover. Open reference areas were defined as areas 1 m from the canopy edge with no canopy (Figure A5).

For the lidar flights during the accumulation season, the average SWE of all 1-m pixels within a 30-m grid cell was taken to represent the target SWE (x), and the average SWE of the open reference 1-m pixels within that same 30-m grid cell was taken to represent the reference SWE (R). The details of the open reference approach are explained in Appendix A and match the Varhola et al. (2010) framework. Low elevation areas (<2,100 m) were excluded from the 2016 and 2022 analyses due to ablation; ablation removes the accumulation signal. We refer to the final metric from Equation 1 as delta accumulation (DSnowAc).

To calculate ablation, we took the SWE loss between each ablation season flight to produce early season (March-April) and late season (April-May) ablation metrics at 1-m resolution. We limited early season ablation data to lower elevations (<2,100 masl) and late season ablation data to higher elevations (>2,100 masl). Because of the limited temporal resolution of these data, if a pixel had no SWE, we could not be sure when that pixel ablated completely. Thus, we excluded all snow-free data, in addition to any areas that experienced accumulation.

For the ablation flights, we modified Equation 1 to create a normalized difference ablation metric (delta ablation, or DSnowAb).

$$y = 100 \cdot \left(\frac{x_i - x_f}{x_i} - \frac{R_i - R_f}{R_i} \right) \quad (2)$$

Where "i" and "f" identify the SWE from the initial and final lidar flights, respectively, within the ablation period.

Random Forest Analysis

We used the Random Forest (RF) machine learning tool implemented through the Ranger package in R to calculate the controls on snowpack accumulation and ablation. RF classifiers use a set of regression trees created using bagged samples from a training dataset. We chose to use a RF because it is an ensemble classifier that can be used with multi-modal data and accounts for covariance in the input variables, and it has been previously used to understand the impact of canopy cover on snowpacks (Krogh et al., 2020, Lewis et al., 2023).

We experimented with several forest structure metrics based on height and lidar point density, and narrowed target metrics based on both preliminary RF runs and knowledge about specific density metrics that have been found to be important in this region . See Table A3 and Figure A3 for details about tested metrics.

We performed RF analyses with [?]y determined from Equation 1 and Equation 2 as the response variables (See Appendix A for more details on RF hyperparameters). Predictor variables for the space-for-structure approach remained the same: elevation, northness, eastness, fVEG, openness, and LAI'.

Decision Support Tool

Based on the results of the RF models, we identified a series of "response" thresholds from slope changes in plots of select predictor variables. Thresholds represent areas where thinning impacts snowpack response (specifically DSnowAc response) either positively (more accumulation) or negatively (less accumulation). We incorporated the results into a simple decision support tool for stakeholders to make informed decisions about forest management. The goal was to capture forest structure thresholds that could be used to target forest structures for thinning. Using the Sagehen Project as a natural experiment, we tested these thresholds against historically disturbed areas to evaluate the effectiveness of thinning on snowpack resilience. We expanded response criteria classification to a larger area covering the eastern extent of the 2014 NCALM flight with similar existing vegetation types (EVT) to SCB (from https://www.landfire.gov/evt.php) to demonstrate how this method could be scaled. The study domain was dominated by coniferous vegetation, aggregated based on the collapsed vegetation type name and physiognomic classification. This allows us to qualitatively assess how broad-scale patterns align with finer-scale patterns and investigate how prior management and disturbance correlates with response classification.

Results

Spatial Patterns of Snow and Forest Structure

Forest structure metrics are highly correlated (Figure A3, Figure 4). LAI', fVEG, and canopy density tend to increase with elevation and northness. Openness shows the opposite trend, decreasing with elevation and northness (Figure A3). Following expected terrain relationships, absolute SWE is greater at higher elevations on more northern-facing slopes in all three accumulation flights (Figure 5). Lower elevations have steady decreases in SWE in denser canopy, but these relationships become less distinct at higher elevations (Figure A6). The relationships between SWE and terrain are nonlinear and in agreement with previous findings (e.g., Kirchner et al., 2014; Tennant et al., 2015; Varhola et al., 2010) showing that areas with lower

SWE tend to be more variable in terms of fVEG and northness, particularly at higher elevations. R-squared values for SWE-elevation regressions are 0.51, 0.68, and 0.43 and slopes are 0.05, 0.19, and 0.09 for the 2008, 2016, and 2022 flights, respectively. R-squared values for SWE-fVEG regressions are 0.12, 0.09, and 0.02 and slopes are -23, -58, and -12 for the 2008, 2016, and 2022 flights, respectively. We calculated that $p < 0.001$ for all models (Figure A9).

"Open Reference Site" Approach

A space-for-structure approach allows us to isolate the effects of vegetation structure by analyzing differences within 30-m grids of up to 900 1-m pixels that we assume experience homogeneous precipitation and the same terrain. We isolate both coarse (fVEG) and fine (LAI' and openness) forest structures using lidar datasets. This approach is applied across three accumulation flights (2008, 2016, and 2022) and two ablation periods (March to April and April to May, 2016).

Accumulation

DSnowAc patterns from SCB are in general agreement with data used in Varhola et al. (2010). DSnowAc decreases (becomes more negative) with an increase in fVEG, indicating that open areas accumulate more snow relative to average 30-m grid cell values (Figure 7; Figure A7). A linear regression of DSnowAc and fVEG shows greater variability and shallower slopes (-0.23, -0.37, and -0.15 for the 2008, 2016, and 2022 accumulation flights, respectively) than the data found in the Varhola et al. (2010) meta-analysis (-0.37; Table 1).

The RF models have varying levels of skill, with R-squared values of 0.72, 0.62, and 0.16 for the 2008, 2016, and 2022 flights, respectively (Table 2). Forest structure metrics explain a greater amount of variance in the model than terrain metrics (Figure A10). Partial plots of snow accumulation predict DSnowAc values between -4% and -20% per 100% change in fVEG and show that on average the forest sites accumulate less snow than open reference sites (Figure 9). A larger absolute DSnowAc indicates that the discrepancy between open and total grid cell SWE is increasing. In this study, we emphasize patterns consistent across select flights. For the 2008 and 2016 flights, fVEG and LAI' have the greatest importance on the RF models with about three times as much influence as terrain variables (Figure A10). There are distinct ranges of influence where certain variables predict greater change in DSnowAc. When fVEG < 0.3, we predict consistent decreases of ~5% snow accumulation. At fVEG values > 0.3, these patterns become more variable, and decrease steeply until fVEG ~0.7, where the relationship becomes weaker but continues to predict decreasing DSnowAc of around -15%. Qualitative thresholds can be observed for both LAI' and openness as well; DSnowAc maintains a maximum around -10% until openness reaches -2.5. A sharp decrease in DSnowAc is predicted until a minimum threshold at around -17% DSnowAc and an openness index of 0 (indicating gap diameter similar to canopy height). DSnowAc shows a steep decreasing trend with LAI', from DSnowAc around -4% at an LAI' of 0 to a DSnowAc minimum around -11% where LAI' is 0.2 (Figure A11). Northness and eastness showed inconsistent results with low importance and no clear trends across the flights (Figure A15; Figure A16). However, the 2008 flight, which best captures accumulation at lower elevations, indicates that southern-facing slopes have a greater difference between open and under-canopy accumulation than other aspects (Figure A14).

Response zones are chosen to quantify snowpack response to canopy removal based on the thresholds identified above (Figure 9). Low response zones are expected to experience the least amount of change post-canopy loss, or post-treatment; high response zones are expected to benefit snow the most. Areas with lower absolute values of DSnowAc (values that approach zero) are typically locations with low density canopy where we would expect greater total accumulation compared with areas with dense canopy and more negative DSnowAc values. Using this framing, we qualitatively identify high (fVEG$>$0.6 and openness$<$-2.5), low (fVEG$<$0.3 and openness$>$0), and moderate (all remaining fVEG and openness values) snowpack response to canopy loss. Low DSnowAc response areas are primarily at higher elevations, often in the steeper terrain, whereas high response areas tend to be at lower elevations and closer to the valley floor (Figure 6) due

to pre-existing patterns in vegetation structure (Figure 4). These response zones show clear differences in average DSnowAc from the space-for-structure approach of ~0, -10, and -30% across low to moderate to high response areas, respectively. Low response areas accumulate more absolute SWE (60 cm in low-response areas vs. 40 cm in high response areas), indicating they would not benefit as much from canopy removal (Figure 10).

The response zones determined through our expanded analysis show clear patterns with previous management and, particularly, forest fires (Figure 11). Areas that have been previously burned are dominated by Ponderosa Pine forest and shrub conversion and have low response classifications. High response areas tend to be forests containing Douglas, Grand, and White Fir. SCB is dominated by moderate response areas, with the proportion of high response areas in planned treatment zones (compared to low-response areas) increasing post-2014.

Ablation

Both DSnowAb metrics show weak increasing linear trends with fVEG and have R^2 values of 0.12 and 0.35 for the March-April and April-May flights, respectively (Figure 8). These relationships indicate that an increase in fVEG leads to greater total ablation relative to the open reference sites.

Elevation explains most of the variance in the RF model for the early season ablation (March-April), followed by fVEG and LAI' (RF r-squared of 0.52; Figure A12). DSnowAb increases as elevation, fVEG, and LAI' increase. An increase in openness predicts a general decrease in DSnowAb, indicating that sites with more openness show more similarity between ablation in the open and ablation under the canopy. fVEG also controls late season ablation (April-May). fVEG and openness explain most of the variance for late season ablation. High DSnowAb response regions emerge between openness values between -3 (gap diameter 1/20 average tree height) and 0 (gap diameter and tree height are equal) and fVEG values between ~0.5 and 0.9 (Figure A13).

Discussion

Comparison with the Varhola et al. (2010) Framework

Maximum snow accumulation has a negative relationship with increasing fVEG using our "open reference site" lidar-based approach, which aligns with the meta-analysis of Varhola et al. (2010). Our approach takes advantage of the lidar point density to compare large scale (30-m) snow distributions with a nearby open reference location (Figure A5), which controls for factors such as precipitation and terrain. However, a limitation of this approach is that the "open reference" area implicitly depends on the amount and arrangement of vegetation (e.g. not all open 1-m areas are the same). Using the flights that best approximate maximum snow accumulation across three years (i.e. the least ablation at lower elevations), we find a linear trend in relative snow accumulation between fully open and 100% fVEG, with differences of 23% in 2008 and 37% in 2016 (R^2 of 0.72 and 0.62, respectively). These slopes are either similar or smaller than those from Varhola et al. (2010), who calculated a slope of 0.37. We see stronger relationships in February 2008 but a lower slope (Figure 7), potentially due to the lack of ablation at lower elevations as compared with March 2016. More lower elevation ablation may accentuate DSnowAc differences because under canopy areas are expected to ablate earlier than open areas in this warmer environment . The correspondence between 2008 and 2016 patterns in DSnowAc with fVEG support the "open reference site" approach and the resulting process inferences we describe below. A random forest model demonstrates that fVEG accounts for the most variation of any predictor variable (fVEG, openness, LAI', northness, elevation) in two of the accumulation models. The RF results show weaker effects when fVEG is below ~30%. The shallower slopes in the RF partial plots (Figure 9; ~10% change in DSnowAc for 100% change in fVEG) compared with the linear relationships suggest the importance of factors besides fVEG (discussed more in Section 4.2).

Our "open reference site" approach predicts greater ablation with increasing fVEG, and thus reductions in ablation rates with canopy removal, which is the opposite of the relationships found by Varhola et al. (2010). However, our results are consistent with process-based studies in warmer climates, where high levels of longwave radiation from trees may overcome the decreased solar radiation in dense forests, especially on shaded north facing slopes Our results demonstrate a need to refine the Varhola et al. (2010) model of ablation for different climates. Steep north-facing slopes may not receive as much increase in solar radiation after thinning compared to flat areas, which would strengthen the signal of higher ablation with higher fVEG in these areas. Greater under-canopy ablation occurs from a combination of the timing of the ablation season (March-May, when solar irradiance is relatively low) and trees that emit enough longwave radiation to dominate energy fluxes . We find an average of ~15% change in ablation for 100% change in fVEG for the March-April and April-May periods (R^2 of 0.13 and 0.34, respectively in Figure 8). Partial plots in the RF model also show positive relationships with fVEG and ablation rate but indicate that there is little effect when fVEG is below ~30% (Figure A13). Ablation rates calculated between two lidar flights are different than season-long ablation metrics used by Varhola et al. (2010). In particular, the lidar-based ablation metrics are affected by snow accumulation during the ablation season, variation in precipitation amount, cold content, energy inputs, and other factors that are highly spatially variable (Figure A3). We attempt to mitigate these issues by using early season (lower elevation) and late season (higher elevation) ablation windows and controlling for initial SWE in each case. However, opportunities exist to improve our method to better utilize ablation information by including distributed snow disappearance estimates with modeling or optical remote sensing. An increasing number of open-source, multi-temporal lidar datasets, collected by ASO for example, in recent years presents an opportunity to repeat these methods across the Sierra Nevada and into domains, like Colorado and Utah, that may show different results due to a variety of energy balance dynamics. Importantly, to be the most useful for this method, these flights must be paired with timely, high point-density, snow-off lidar as well.

Role of Finer-Scale Forest Structure and Terrain on Snow Dynamics

The predictor importance shows that fVEG, LAI', and openness are more important than terrain metrics (elevation, northness, and eastness) for predicting our DSnowAc metric in the RF model (Figure A9). The importance of these vegetation metrics was clearly shown by our "open reference site" approach since analyses of raw snow accumulation data would fail to disentangle the role of vegetation from the strong influence of elevation and snowfall spatial patterns (Figure 4 and Figure 5). The partial plots from the RF model consistently show a non-linear effect on accumulation from LAI' and openness, as compared to a more linear relation with fVEG. Overall, our results imply that vegetation has the largest role in reducing snow accumulation when fVEG is high (>0.6), openness is low (vegetation height [?] canopy gap diameter), and LAI' is high (>0.25). Inversely, these results indicate that a canopy gap diameter to vegetation height ratio <1 optimizes accumulation, in general support of earlier studies that demonstrated maximum shading across the gap when nearby canopy height is comparable to the gap diameter (i.e. openness ratios <1) . Conversely, partial plots for terrain effects on accumulation and ablation have shallower slopes, with mixed slopes across flights suggesting weaker controls (FigureA14-A18). Our results match Krogh et al. (2020) and Lewis et al., (2023), who used the SnowPALM model to conclude that lower-elevation, south-facing slopes experience post-thinning increases in accumulation.

We also show the importance of fine-scale forest structure controlling ablation rates, and promoting snow retention following thinning, despite limitations in our random forest analysis. Because of differences in energy environments, elevation is important for predicting DSnowAb, whereas fVEG, openness, and LAI' are more important for the early ablation season metric. Both early and late season ablation estimates indicate a combined impact of fVEG (lowest ablation at <~50% canopy cover) and openness (lowest ablation where gap diameter is greater than tree height) to promote retention. The similar response of snow accumulation and ablation suggests that forest thinning in dense areas – especially if the thinning creates large gaps rather than uniform density reduction – is likely to slow ablation while increasing accumulation, thereby increasing overall snow retention.

Despite the importance of a coarse (simpler) fVEG metric based only on tree spatial coverage, we find that metrics accounting for vertical lidar point density (LAI') and horizontal and vertical canopy information (openness) help refine predictions of snow-forest interactions. For example, different species of trees often have different LAI' and height, while in forest patches with similar forest species the spacing and orientation of the trees may be different. Similarly, the land use history or resource limitations of the local area could be important for coarse and fine-scale forest structure information (Stephens et al., 2021). It's worth noting that these forest structure metrics are highly correlated across the full domain, but their correlation within elevation bands is more mixed due to more homogeneity in forest species, terrain, land use history, and other factors (Figure 4). fVEG is the most important vegetation metric in our analysis, compared with openness and LAI', is easier to estimate, and matches the linear relationship found in Varhola et al. (2010). Importantly, however, Varhola et al. (2010) did not explore finer scale forest structure information like openness and LAI'. Varhola et al. (2010) also emphasized the inconsistencies between forest structure metrics across studies, which hints at the value of using lidar information to develop repeatable coarse and fine forest structure information.

Management applications and future research directions

While simple linear models capture broad patterns of forest-snow interactions, thresholds at which specific forest structure metrics become important can help refine forest management decisions beyond the current decision-making paradigm that typically does not include benefits to snow water resources. We developed a decision support tool for SCB, and extrapolated that to a landscape scale, by defining qualitative thresholds in fVEG and openness that correspond to high, moderate, and low response of SWE to potential thinning. The Sagehen Project was a mixture of mechanical thinning and prescribed fire that was planned to address wildlife and fire concerns and resulted in the fragmented treatment areas shown in Figure 1. We find near zero DSnowAc (˜0%) and more absolute SWE (˜50 cm) in the low response areas of SCB, suggesting that our threshold method has identified areas with little response to thinning or other canopy removal. These areas account for a small portion (˜7% in 2014) of the total domain, suggesting medium and high response areas were widespread across SCB prior to thinning from the Sagehen Project. The high response areas had a delta SWE of around -25% and lower absolute SWE of ˜30 cm. Only 29% of the treated areas as part of the Sagehen Project thinning were high response areas (pre-thinning), while 27% were moderate response. While the resilience of snowmelt-derived water resources was not an explicit priority for the Sagehen Project, it illustrates the potential co-benefits of simultaneously managing forest fire reduction, wildlife habitat, and snow retention . Our decision support tool offers both a retrospective means to assess restoration effectiveness (as done in the Sagehen Project area), as well as a tool for proactive planning efforts.

One of the key advantages of our results for decision support purposes is that it can be extrapolated to larger domains of similar climate and forest conditions or re-developed in new areas with different snow conditions (e.g. colder and windier) that have existing snow-on and snow-off lidar datasets. To demonstrate the scalability of our results for decision support, we extended our low, medium, and high response mapping to an 800 km^2 landscape-scale area with planned forest restoration by the USFS. Lidar analyses showed that treated areas had a higher relative proportion of low response zones compared to areas that had not yet been treated, suggesting that treatment planning was optimizing areas for increased snow retention. The increase in the treatments in high response zones after 2014 suggests that this type of lidar-based analysis could have been used proactively to plan treatments for maximum snow effects. Areas near SCB that have burned in recent years (Figure 11b), especially those that have converted to shrub cover, show a much higher proportion of low response areas compared to surrounding unburned and un-thinned forestland. This difference suggests that the fires were effective at changing forest structure in a manner that would increase snow accumulation and retention, but that land cover conversion from forest to shrub may have impacts not estimated with our decision support tool. While wildfires may increase ablation due to black carbon reducing albedo several years post-fire , other studies have shown that reductions in canopy cover from fire can provide net benefits to snowpack and streamflow in the Sierra Nevada . Our method does not consider the effects of fire or other processes that disturb the snow albedo or energy budgets beyond physical changes

in forest structure. The simplicity of our methods suggests that replicating our method in different forest types, different forest restoration treatments, and across a range of climates with lidar data coverage could yield both process insight and new decision support tools.

Conclusion

We present a new lidar-based method that furthers our understanding of effects of forest disturbance on snow accumulation and ablation and translates that into a decision support tool. Our novel and open-source methods for processing high-resolution, spatially-distributed lidar data identify forested zones which are most likely to experience increased snowpack water storage following canopy removal from forest treatments. Our "open reference site" analyses motivated by the Varhola et al. (2010) meta-analysis, confirms a linear predictive relationship between coarse-scale forest structure metrics (i.e. fVEG) and snow accumulation. However, our method utilizing thousands of "reference sites" provides new insight about thresholds in fine-scale forest structure metrics (i.e. openness) that were not possible with previous observational techniques. Our analysis allows us to isolate the fine-scale forest structure metrics using widely available airborne lidar datasets, thereby creating opportunity to understand climate-driven differences in snow retention across multiple sites. Moreover, cross site analysis that spans climate and snowpack gradients could yield truly novel insights into the underlying processes controlling snow accumulation. Ablation dynamics and pre-post disturbance analyses presented methodological challenges, primarily from temporal limitations in lidar collections across the large elevation gradients. Despite a detectable shift towards less ablation with lower fVEG, an improved method for calculating ablation using multi-temporal lidar across large elevation gradients would be valuable. Lidar data collections in the snow accumulation season have the potential to inform decision support tools , but have more limitations in detecting post-disturbance change, while inter-annual variability limits pre versus post disturbance analyses. Consequently, lidar data collections need to be tailored to local conditions (e.g. low and high elevation collections) and done in close coordination with local management agencies to maximize utility for forest restoration planning.

Acknowledgements

The authors would like to thank Kat Bormann and the rest of the ASO team for their guidance in acquiring and processing lidar datasets. Thanks also to collaborators at Open Topography and NCALM for the opportunity to collect and present (through open-source platforms) high-resolution, spatially-distributed lidar data. This study was funded by Proposition 68 the Sierra Nevada Conservancy through the California Tahoe Conservancy and the U.S. Forest Service Pacific Southwest Research Station, Grant 1149, project P68IP001. A. Harpold and C. Piske were partially supported by NSF EAR #2012310 and EAR #1723990. C. Piske was partially supported by the Nevada NASA Space Grant Consortium (NNX15AI02H).

References

Tables

Table 1: Linear Regressions, Delta Snowpack Accumulation/Ablation vs. Fraction of Vegetation

Date	P-Value	R-Squared	Residual Std. Error	Slope
02/10/2008	<0.001	0.63	4.1	-0.23
03/26/2016*	<0.001	0.31	11.6	-0.34

Date	P-Value	R-Squared	Residual Std. Error	Slope
03/26/2016	<0.001	0.23	15.4	-0.37
03/21/2022*	<0.001	0.058	12.8	-0.15
03/21/2022	<0.001	0.016	13.5	-0.084
March-April	0.01	0.13	10.4	0.17
April-May	<0.001	0.34	3.52	0.13

Note: *Elevations limited to >2100m

Table 2. Random Forest Model Results, "Open Reference Site" Analysis

Date	OOB R-Squared	OOB MSE
02/10/2008	0.72	12.21
03/26/2016*	0.62	73.28
03/21/2022*	0.16	157.44
March-April	0.51	63.88
April-May	0.72	73.28

Note: *Elevations limited to >2100m

OOB – out of bag, MSE – mean squared error.

Response variables are DSnowAc and DSnowAb. Predictor variables include elevation. fVEG, LAI', openness, eastness, and northness.

Figures

Figure 1. Sagehen Creek Basin, located in the northeastern Sierra Nevada. The area of interest (black outline) shows the study domain given available lidar and modeled snow density. a. The elevation profile spans ~1800 to 2800 meters, increasing to the southwest. b. Northness shows steep slopes to the southwest. c. The thinning project summary shows proposed thinning boundaries overlaying a canopy height model (CHM) in meters, which align well with the fraction of vegetation (fVEG) difference between the pre- and post-thinning flights (d).

Figure 2. SNOTEL SWE values compared with flight dates (vertical dashed lines) used in this study for water year (a) 2008, (b) 2016, and (c) 2022. Orange = Independence Lake SNOTEL Site (541), Black = Independence Camp SNOTEL Site (539), Blue = Independence Creek SNOTEL Site (540).

Figure 3. (a) Example image displaying the lidar snow-on classification with an example subsection of a lidar grid cell (tan = ground, green = vegetation, blue = snow surface). The bottom color bar aligns with the correct canopy cover class as classified from the height strata (dark blue = open, light blue = short canopy, dark green = tall canopy, light green = understory). The black zones indicate that the area above would be removed from the analysis, either because there are points between 1.5-3 m or because the snow is not >0.3 m above the vegetation surface (note: not to scale and point cloud colors do not correspond with classification colors). b. Vegetation classification output. The refined classification includes short and understory classes, allowing us to include shorter vegetation types if the snow depth is [?] 0.3 m above the vegetation. c. Snow-depth classification example for the 04/17/2016 flight.

Figure 4. Spatial distribution of pre-disturbance forest structure metrics across the area of interest, colored

by northness, where negative values indicate south-facing slopes. Box plots show quartiles with the horizontal bar representing the median value. Higher elevations tend have denser canopy on northern-facing slopes.

Figure 5. Spatial distribution of SWE across the domain. We see greater SWE at higher elevations and more northern-facing slopes.

Figure 6. Median DSnowAc (shown by horizontal lines within each box plot) is always below zero, indicating greater accumulation in open areas. The spatial distribution of DSnowAc across the domain is varied with a more pronounced difference at lower elevations on more northern-facing slopes in 2016 and more muted effects in 2008 and 2022.

Figure 7. DSnowAc against fVEG for the a. NCALM flight from 02/10/2008. b. ASO flight from 03/26/2016 c. NCALM flight from 03/21/2022. Lidar points are colored by density with darker blue = greater point density. Black points show the Varhola et al. (2010) data.

Figure 8. Normalized DSnowAb against fVEG for both early (a) and late (b) season ablation show a weak positive relationship, with the differences between forested and open sites increasing (becoming more positive) with increasing vegetation.

Figure 9. Annotated partial plots showing the response area determination. Higher pre-disturbance fVEG areas are identified as high response areas because thinning would lead to a pronounced increase (positive response) in DSnowAc whereas lower pre-disturbance Openness (ln[gap diameter/mean tree height]) areas are identified as high response because thinning would lead to a pronounced decrease (negative response) in DSnowAc.

Figure 10. Predicted response classes based on the Random Forest results. Shading shows areas that are predicted to experience a low (light purple), moderate, or high (dark purple) response to treatment. a. The spatial distribution of these maps on top of actual treatments, shown both as planned treatment outline (dotted black line) and the delta fVEG raster. b. Snow accumulation dynamics across all three flights and predicted response classes.

Figure 11. An expanded response analysis using the 2014 lidar flight. The LANDFIRE EVT map (a. and c.) shows that the domain is dominated by Ponderosa Pine Forests, which are also primarily where areas are impacted by fire. Moderate response zones account for the majority of the domain, and high response areas are concentrated between Douglas/Grand/White Fir and Ponderosa Pine Forests (c.). Treatment and burned areas overlain on an expanded response map show that low response areas overlap with burned areas (b.) and taking the area of pixels per each date range, the proportion of low response areas increases as the treatment dates become more recent (e.g. 2007-2014). Planned treatment areas (2014-2024) show an increase in high response areas.

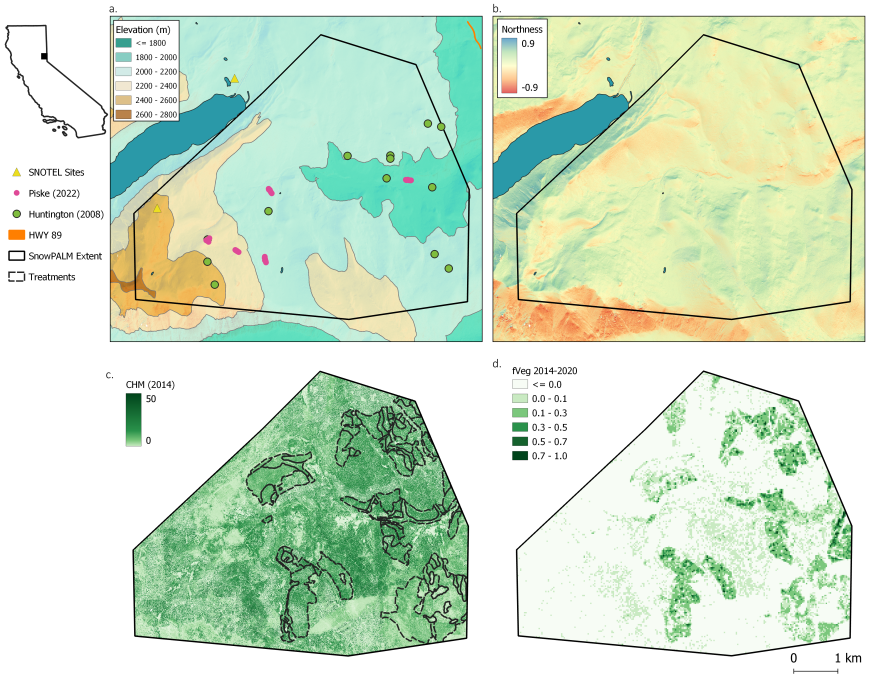

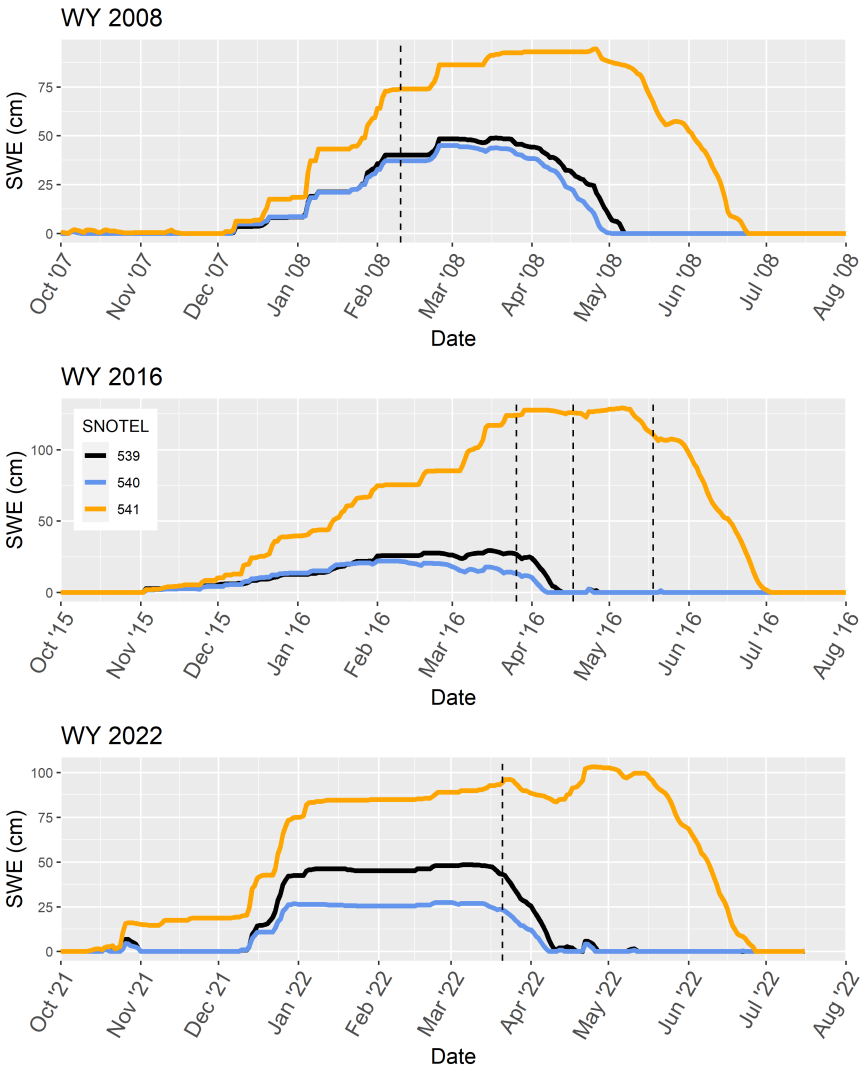

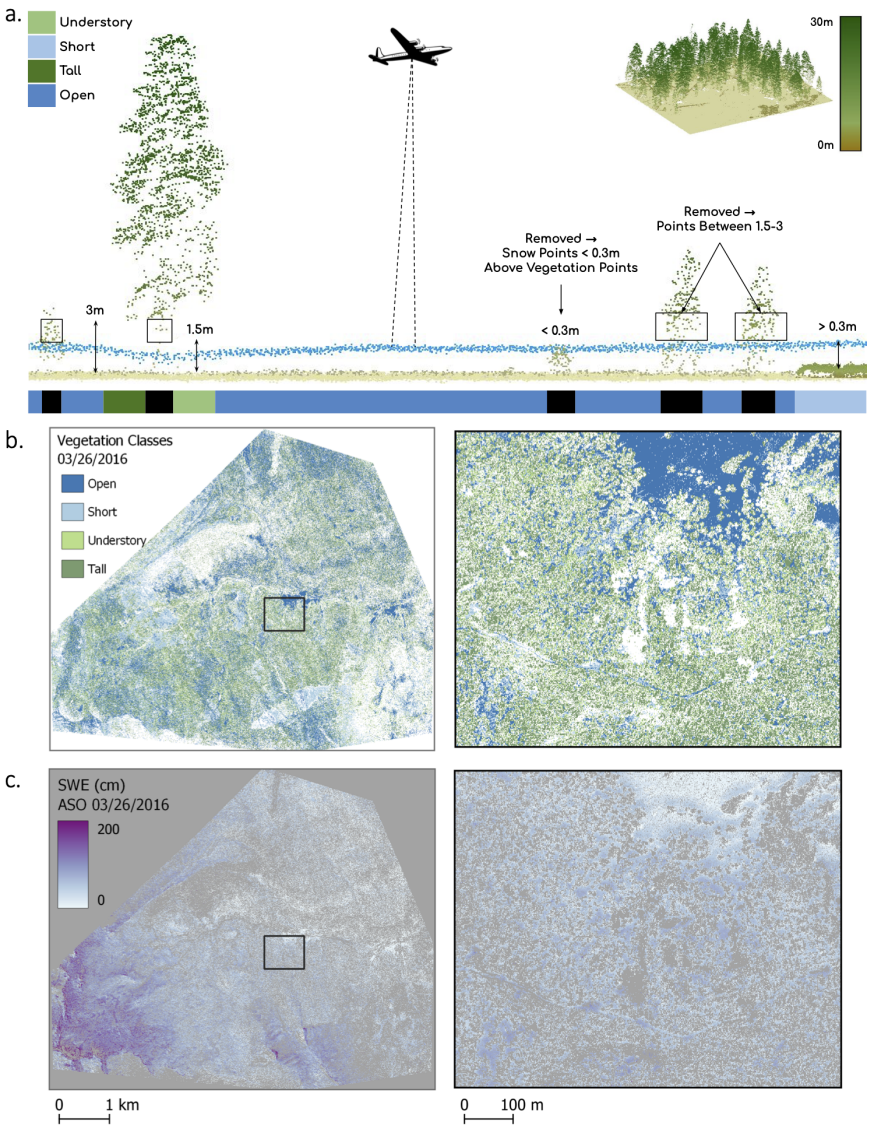

Hosted file

Fig. 4.docx available at https://authorea.com/users/793695/articles/1101648-lidar-derived-forest-metrics-predict-snow-accumulation-and-ablation-in-the-central-sierra-nevada-usa

Hosted file

Fig. 5.docx available at https://authorea.com/users/793695/articles/1101648-lidar-derived-forest-metrics-predict-snow-accumulation-and-ablation-in-the-central-sierra-nevada-usa

Hosted file

Fig. 6.docx available at https://authorea.com/users/793695/articles/1101648-lidar-derived-forest-metrics-predict-snow-accumulation-and-ablation-in-the-central-sierra-nevada-usa